Pharmaceutical Research, Vol. 24, No. 5, May 2007 (© 2007)
DOI: 10.1007/s11095-006-9205-0

Research Paper

Miniaturized Assay for Solubility and Residual Solid Screening (SORESOS) in Early Drug Development

Nicole Wyttenbach,[1,3] Jochem Alsenz,[1] and Olaf Grassmann[2]

Received August 30, 2006; accepted December 4, 2006; published online March 20, 2007

Purpose. The aim was to develop a miniaturized method for solubility and residual solid screening of drug compounds in aqueous and non-aqueous vehicles in early drug development.
Methods. Different crystal modifications of caffeine, carbamazepine, and piroxicam were added into 96-well filter plates and solubility was determined in 100 µl of 17 pharmaceutical vehicles. After filtration, drug concentration was determined by Ultra Performance Liquid Chromatography™ (UPLC). Residual solid drug in the filter plates was analyzed by high-throughput (HT) transmission X-ray Powder Diffraction (XRPD).
Results. HT XRPD analysis revealed solid form conversions of all compounds during solubility determination, e.g., formation of hydrates in aqueous vehicles (caffeine, carbamazepine, piroxicam) or conversion of a metastable crystal form to the stable form (caffeine). Drug solubility was strongly dependent on the crystal modifications formed during the solubility assay.
Conclusions. The new assay allows the simultaneous, small scale screening of drug solubility in various pharmaceutical vehicles and identification of changes in solid form. It is useful for the identification of formulations and formulation options in non-clinical and clinical development.

KEY WORDS: polymorphism; high-throughput; solubility; ultra performance liquid chromatography (UPLC); X-ray powder diffraction (XRPD).

INTRODUCTION

Pharmaceutical profiling of drug candidates in the late lead optimization and clinical candidate selection phase is of utmost importance in the pharmaceutical industry to identify the drug candidate with the best probability of successful development (1–4). Profiling activities include drug solubility, stability, compatibility, and permeability studies as well as salt- and polymorph screening and selection. In this phase, the determination of drug solubility is important for the identification of promising formulation approaches for preclinical *in-vivo* studies (pharmacodynamic, pharmacokinetic, and toxicological studies) and for the estimation of the "developability" of drug candidates, particularly in case of poorly soluble compounds.

At the drug discovery-development interface, a broad solubility screening in various buffers, simulated intestinal fluids, pharmaceutical solvents (oils, surfactants, co-solvents, etc.), and liquid formulation vehicles should be performed for the remaining 1–10 drug candidates. Since at this stage of development, typically only 100–500 mg of compound is available for pharmaceutical profiling activities, several miniaturized assays for solubility measurements in pharmaceutical vehicles have been suggested. Chen *et al.* (5) established a 96-well high-throughput (HT) combinatorial approach at a 100 µl scale for the development of a Cremophor-EL free intravenous paclitaxel formulation. In their set-up, drug solubility is analyzed by turbidity measurement using a UV plate reader at 500 nm to detect potential drug precipitation. Another assay, developed by Chen and Venkatesh (6), uses a miniature device for aqueous and non-aqueous solubility measurements based on a multichannel cartridge pump. Drug slurry is filled into the tubing, continuously circulated inside through a syringe filter and finally drug in the collected filtrate is analyzed by High-Pressure Liquid Chromatography (HPLC). Recently, a new partially automated solubility screening (PASS) assay for early drug development was published by Alsenz *et al.* (7). In this assay, the solubility of drug compounds in aqueous and non-aqueous solvents is determined in a 96-well system up to 100 mg/ml drug concentration at a 40 to 80 µl scale. Solid–liquid separation is performed by filtration and drug concen-

[1] Department of Preclinical Research, Pharma Division, F. Hoffmann-La Roche Ltd., Bldg. 093/724, CH-4070, Basle, Switzerland.
[2] Molecular Structure Research, Pharma Division, F. Hoffmann-La Roche Ltd., CH-4070, Basle, Switzerland.
[3] To whom correspondence should be addressed. (e-mail: nicole.wyttenbach@roche.com)

ABBREVIATIONS: CAF, caffeine; CBZ, carbamazepine; DSC, differential scanning calorimetry; FaSSIF, fasted state simulated intestinal fluid; FeSSIF, fed state simulated intestinal fluid; FT-IR, Fourier Transform IR spectroscopy; Mixed micelles (200 mM G/L), aqueous vehicle containing 200 mM glycocholic acid and 200 mM lecithin; PCTE, polycarbonate, track-edged; PXM, piroxicam; SGF, simulated gastric fluid; SORESOS, solubility and residual solid screening; TGA, thermo gravimetric analysis; UPLC, Ultra Performance Liquid Chromatography™; XRPD, X-ray Powder Diffraction.

tration in the filtrate is determined by Ultra Performance Liquid Chromatography™ (UPLC) (8,9). A head-to-head comparison of several solubility assays is discussed by Alsenz *et al.* (7).

In HT solubility screening, the residual solids are rarely investigated systematically, although transitions to different solid forms in the presence of liquid pharmaceutical excipients or vehicles have been reported (7,10,11). Many drugs form polymorphs and solvates that can have different physicochemical properties such as melting point, enthalpy of fusion, vapor pressure, density, hardness, color, dissolution rate and that can differ considerably in solubility (12,13). Knowledge of polymorphism of new compounds is normally missing in the very early phase of a project. Since amorphous or thermodynamically unstable crystalline material is often used for initial solubility studies the probability of solid form changes is high. Therefore, a combined screening method for solubility and residual solid on a microscale setting would be of great value. This would, to our knowledge, for the first time allow the correlation of drug solubility with solid state forms in a HT solubility screen. Such an assay focuses on excipient screening for early formulation development and is not intended to replace dedicated HT polymorph screening, that is usually performed in organic solvents in later phases (14–17).

The purpose of this study was the development of such a combined assay for the late lead optimization and clinical candidate selection phase. A miniaturized, medium-throughput assay based on 96-well filter plates was set-up that allows parallel solubility measurement and residual solid screening in aqueous and non-aqueous solvents. It uses UPLC for fast determination of drug solubility in large numbers of pharmaceutically relevant vehicles and HT transmission XRPD for direct detection of solid form changes in residual solids in 96-well filter plates. Transmission XRPD is a robust method for HT analysis because only a small amount of material is needed and variations in specimen height affect the peak positions of low angle peaks less compared to conventional Bragg–Brentano reflection geometry (18,19).

Caffeine, carbamazepine and piroxicam served as model compounds for assay development since they form hydrates and have several polymorphs (20–24). To ensure the validity of the new model, HT solubility results of carbamazepine were compared to solubility data determined with a standard large-volume solubility test.

MATERIALS AND METHODS

Materials

Commercial carbamazepine (CBZ), caffeine anhydrous (CAF) and piroxicam (PXM) were purchased from Sigma-Aldrich Chemie GmbH (Buchs, Switzerland). Caffeine "monohydrate" was from MP Biomedicals, Inc. (Solon, OH, USA). All other chemicals and excipients procured from commercial sources, and were used as purchased without further purification or treatment. Solvents used for UPLC analysis, were of HPLC quality grade.

Composition of Particular Vehicles

Buffer pH 6.5 contained 50 mM sodium dihydrogen phosphate in deionized water adjusted to pH 6.5 with 1 N NaOH. Simulated gastric fluid (SGF) was composed according to Galia *et al.* (25). SGF contained 10 mM HCl, 2 mg/ml sodium chloride, 1 mg/ml Triton® X-100 and had a pH of 2.0. Simulated fasted and fed state intestinal fluids were prepared as previously reported (26). Fasted state simulated intestinal fluid (FaSSIF) contained 3 mM sodium taurocholate, 0.75 mM lecithin and had a pH 6.5. The fed state medium FeSSIF simulated intestinal fluid contained 15 mM sodium taurocholate, 3.75 mM lecithin and had a pH 5.0. The mixed micelles vehicle (200 mM G/L) contained 200 mM glycocholic acid and 200 mM lecithin and was composed according to Teelmann *et al.* (27) without benzyl alcohol and sodium pyrosulfite.

Preparation of Modifications of CBZ, PXM, and CAF

The metastable form I of CBZ was obtained by heating the commercial CBZ (form III) at 170°C for 2 h, as described by Lefebvre *et al.* (28). Alpha-CBZ was obtained by equilibration of 300 mg CBZ form I in 3 ml Labrafil M 1944 CS for 24 h at room temperature. The hydrated forms of CBZ and PXM were prepared by suspending the commercial compounds (5% w/w) in distilled water for 24 h at room temperature in the dark. The residual solids were subsequently dried on filter paper at room temperature for 30 min. The high temperature form I of CAF was prepared by heating the commercial CAF (form II) at 180°C for 16 h in a closed vessel (20).

Solubility Determination by SORESOS

A schematic representation of the newly developed solubility and residual solid screening (SORESOS) assay is

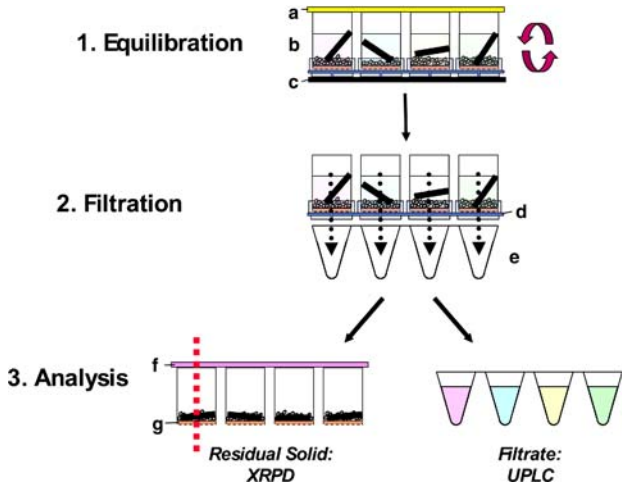

Fig. 1. Schematic representation of the experimental procedure of the solubility and residual solid screening (SORESOS) assay. Experiments are performed in 96-well MultiScreen® Solubility Filter Plates (**b**) sealed with an ELAS™ septum sheet (**a**, *top*) an adhesive aluminum foil (**c**, *bottom*). Drug-vehicle slurries are mixed by head-over-head rotation in the presence of stirring bars, seals are removed, and filtration is performed by centrifugation. Filtrates are collected in a 96-well polypropylene plate (**e**). After filtration, the plate is sealed by adhesive acetate foil (**f**), the underdrain support (**d**) of the filter plate is removed, and residual solid on the filter (**g**) of the plate is directly analyzed by HT transmission XRPD with vertical beam geometry (*dashed line*).

depicted in Fig. 1. Experiments were performed in 96-well MultiScreen® Solubility Filter Plates (product number MSSLBPC10, 0.4 μm modified PCTE membrane, Millipore, Bedford, MA). The bottom of the plate was sealed with adhesive aluminum foil (product number 951023001, Eppendorf AG, Hamburg, Germany) to prevent evaporation of the solvents during equilibration. The compound (10–15 mg per well) was dispensed volumetrically into filter plates using a manual powder dispenser for 96-well plates (Titan Resin Loader System, Spike International Ltd., Wilmington, NC) (3×6 mm, diameter x depth). Single use stirring bars (product number VP711—1, 1.67×2.01×4.80 mm, parylene coated, V&P Scientific Inc., San Diego, CA) and 100 μl of each pharmaceutical vehicle were added. One well per plate containing pure drug served as reference sample for HT XRPD analysis. All experiments were performed in triplicate. Immediately after filling, the plate was sealed by an ELAS™septum sheet (product number 3600805, Zinsser Analytic GmbH, Frankfurt, Germany) using a custom-built clamp device. The drug-vehicle slurries were mixed by head-over-head rotation at 20 rpm for 24 h at room temperature using a Heidolph Reax 2 mixer (VWR International AG, Dietikon, Switzerland). The adhesive aluminum foil and the ELAS™ septum sheet were removed and liquid was separated from residual solid by centrifugation at 3,300 g for 5 min (Heraeus Omnifuge 2.0 RS, Kendro Laboratory Products AG, Zürich, Switzerland). The filtrates were collected in a 96-well polypropylene plate (150 μl twin.tec skirted PCR plate 96, product number 951020401, Eppendorf AG, Hamburg, Germany). After centrifugation, the filter plate was immediately sealed with adhesive acetate foil for microtest well plates (product number 82.1586, Sarstedt Inc., Newton, NC). The plastic underdrain support of the filter plate was removed and the wet substance pellets in the plate were directly analyzed by HT transmission XRPD. Drug contents in the filtrates were determined by UPLC after appropriate dilution of the samples with N-Methyl pyrrolidone (7).

Large-Volume Solubility Experiments

Equilibrium solubilities of CBZ form III were determined in large-volume experiments in triplicate. Excess solid of CBZ form III, a magnetic stir bar and 5 ml of vehicle were added into 20 ml glass vials with screw caps (product 8075-20-H, Infochroma AG, Zug, Switzerland). The closed vials were equilibrated on a ten-place magnetic stirrer (IKA RO 10 Power, IKA-Werke GmbH & Co. KG, Staufen, Germany) at room temperature. 200 μl samples were withdrawn after 14, 20 and 24 h. The samples were filtered with Ultrafree-MC® centrifugal filter devices (product number UFC30HV00, 0.45 μm

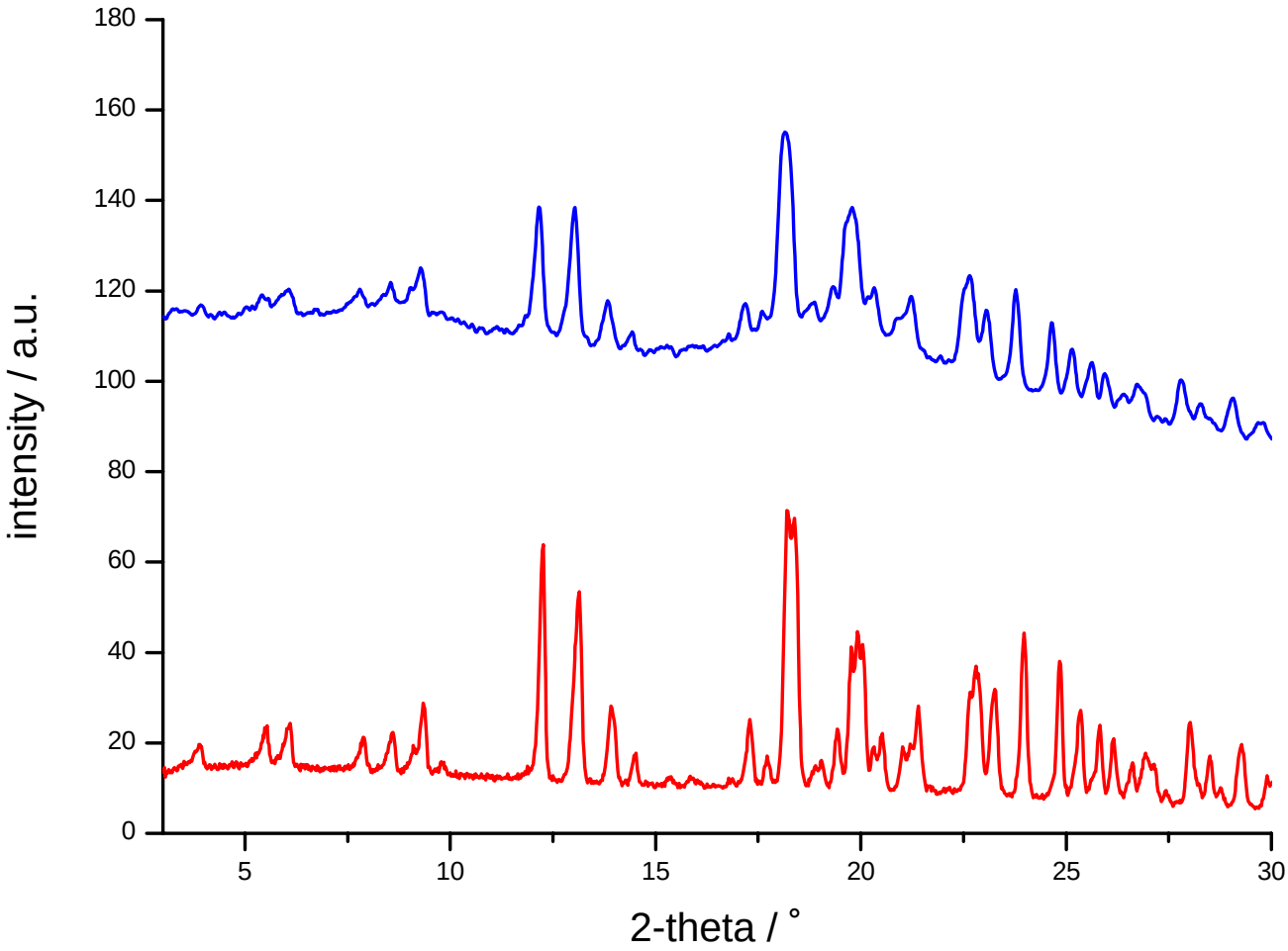

Fig. 2. Overlay of a standard transmission XRPD pattern of CBZ form I (*bottom*) and the corresponding pattern recorded by HT transmission XRPD (*top*).

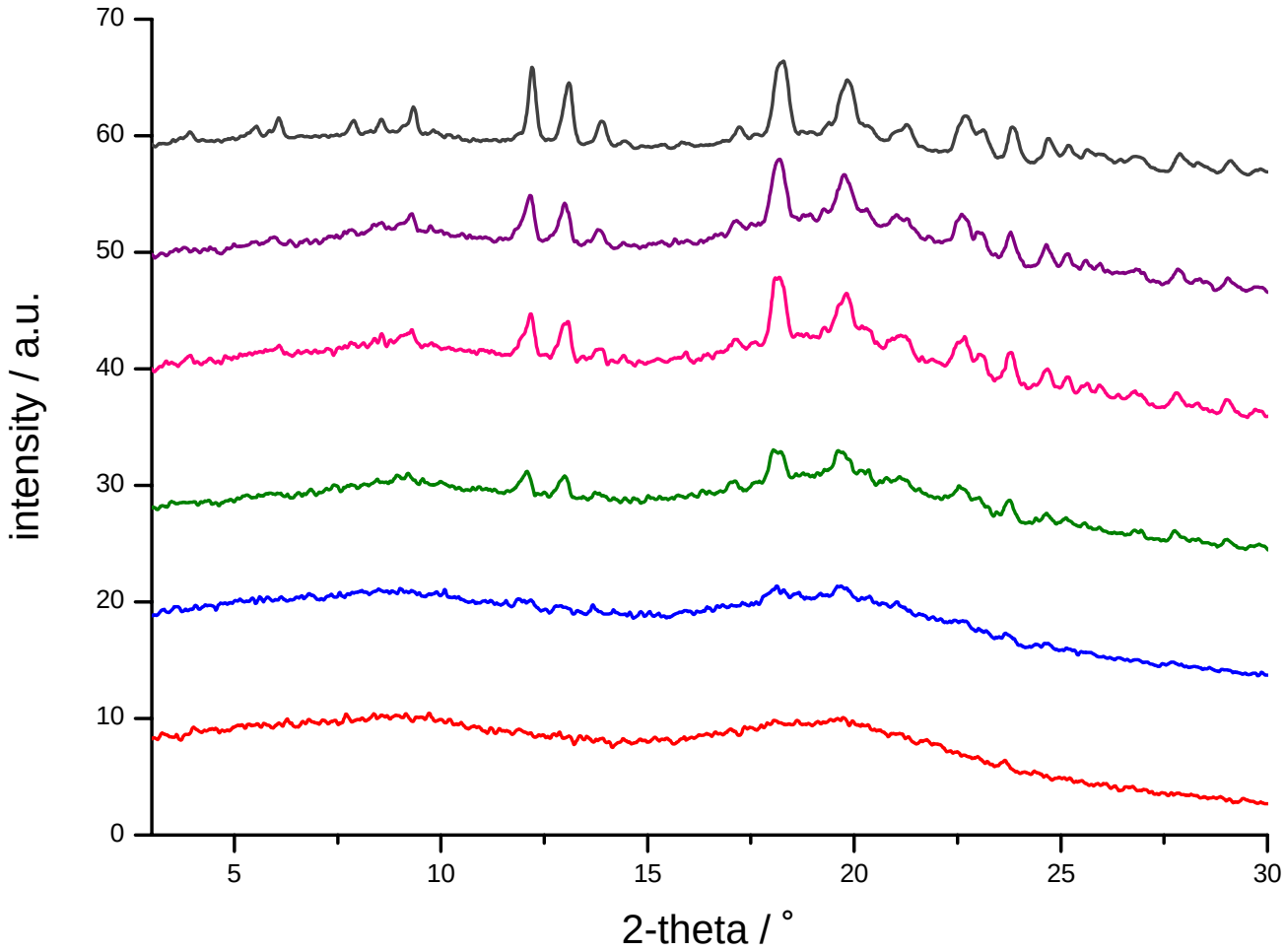

Fig. 3. HT XRPD patterns of wells containing 0.5, 1, 2, 3, 4 and 5 mg of CBZ form I (*bottom to top*). Patterns from wells containing at least 2 mg CBZ allow a clear identification of the crystalline phase.

Durapore PVDF membrane, Millipore, Bedford, MA). The amount of dissolved drug in the filtrate was determined by UPLC. When the final value was in agreement with the previous one, equilibrium was assumed to be reached. The residual solids were analyzed by standard X-ray powder diffraction.

X-ray Powder Diffraction (XRPD)

High-quality reference patterns of CAF, CBZ and PXM were recorded in transmission geometry on a STOE Stadi P diffractometer ("standard method"). The diffractometer is equipped with a primary Ge-monochromator to obtain monochromatic CuKα1 radiation and a position sensitive detector (PSD). The recording PSD step width of 0.5° 2-theta and a measurement time of 40 s per step accumulated to approximately 60 min measurement time. Samples (20 to 30 mg) were prepared between thin foils of cellulose acetate and analyzed without additional processing (e.g., grinding or sieving).

For HT transmission XRPD analysis of 96-well filter plates, a STOE Stadi P Combi diffractometer equipped with primary Ge-monochromator (CuKα1 radiation), imaging plate position sensitive detector (IP-PSD) and 96-well plate sample stage was used. The IP-PSD allowed simultaneous recording of the diffraction pattern both side of the primary beam. HT transmission XRPD data quality was significantly improved by merging both 2-theta ranges using the software STOE WinXPOW. Effects related to poor crystal orientation statistics are reduced by summing up diffracted beam intensities both side of the primary beam. The imaging plate detector was exposed for 10 min to X-ray radiation for each well. Additionally, approximately 1 min was needed for detector read-out and imaging plate erasing. Samples were analyzed directly in the 96-well filter plates without prior preparation and additional processing.

Quality Assessment of HT XRPD Patterns

The quality of the HT transmission XRPD method was assessed by comparing the standard method XRPD pattern of CBZ form I with the pattern obtained from HT XRPD. The minimum amount of sample needed for HT XRPD analysis was determined by measuring wells of a 96-well MultiScreen® filter plate containing increasing amounts of each model compound (0.5, 1, 2, 3, 4, and 5 mg). The plates were sealed with adhesive acetate foil before subjecting to HT XRPD analysis. In addition, HT XRPD measurements of wetted samples were performed. After recording the patterns of the dry samples, 100 µl of olive oil were added to each well. After centrifugation for 5 min at 3,300 g in a Heraeus Omnifuge 2.0

RS (Kendro Laboratory Products AG, Zürich, Switzerland), the plate was sealed with adhesive acetate foil and the oil-wetted samples were analyzed again by HT XRPD.

DSC

A DSC821^e instrument from Mettler-Toledo (Greifensee, Switzerland) was used. The DSC was calibrated for temperature and enthalpy using indium. Nitrogen was used as protective gas (150 ml/min). Samples (2–5 mg) were heated at 5°C/min in aluminum pans with pierced aluminum lids (40 µl, Mettler-Toledo, Greifensee, Switzerland) to temperatures in excess of the reported melting points of the respective compounds.

TGA

A TGA/SDTA851^e instrument from Mettler-Toledo (Greifensee, Switzerland) was used. The instrument was calibrated for temperature using indium and zinc. Nitrogen was used as a protective gas at a flow rate of 100 ml/min. Samples (2–5 mg) were heated at 5°C/min in aluminum pans with pierced aluminum lids (40 µl, Mettler-Toledo, Greifensee, Switzerland) to 300°C.

FT-IR

Reference samples were analyzed by Fourier Transform IR spectroscopy using a Nicolet 20SXB spectrometer (32 scans at 2/cm resolution). A Nujol suspension containing approximately 5 mg of sample was prepared between two sodium chloride plates and measured in transmittance.

UPLC

Analysis was performed on a Waters Acquity™ Ultra Performance Liquid Chromatographic system, equipped with a 2996 Photodiode Array Detector and an Acquity UPLC™ BEH C18 column (2.1×50 mm, 1.7 µm, particle size, Waters, Milford, MA). Mobile phase A and B consisted of 0.1% triethylamine in deionized water adjusted to pH 2.2 with methanesulfonic acid and acetonitrile, respectively. The flow rate was 0.75 ml/min and total run time was 1.2 min. The linear gradient and the wavelength of detection were compound specific.

RESULTS

Quality of HT Transmission XRPD Measurements

The quality of HT XRPD measurements was evaluated by comparing the standard XRPD pattern of CBZ form I with a pattern obtained from HT transmission XRPD. The angular resolution of the X-ray pattern obtained from HT transmission XRPD was lower and the background was higher than for the standard pattern (Fig. 2). However, the peak position and relative intensities of characteristic peaks of CBZ form I corresponded well to the fingerprint obtained from the standard XRPD method and phases are selectively identified by their characteristic peaks.

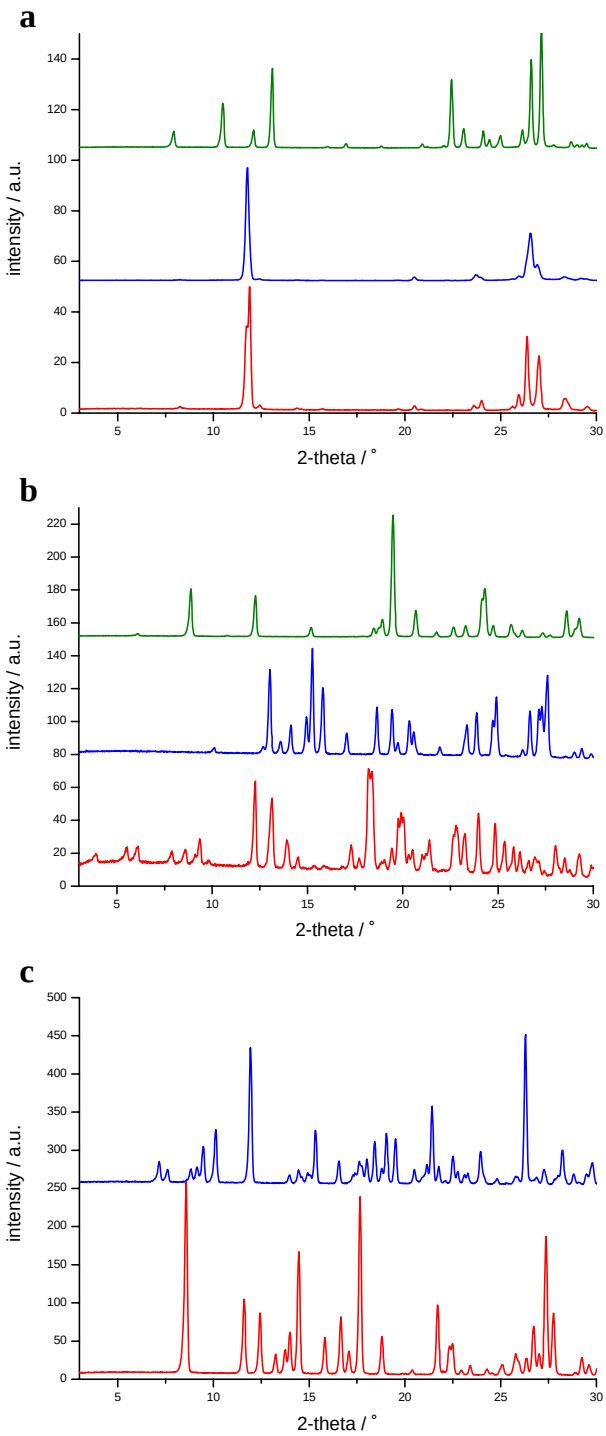

Fig. 4. Standard XRPD reference patterns of different polymorphs of the model compounds: **a** Caffeine (CAF): form II (*bottom*), form I (*middle*), and hydrate (*top*). **b** Carbamazepine (CBZ): form I (*bottom*), form III (*middle*), and dihydrate (*top*). **c** Piroxicam (PXM): form I (*bottom*) and monohydrate (*top*).

The HT XRPD patterns of wells containing different amounts of CBZ form I show a good correlation between the amount of sample and the intensity of characteristic peaks (Fig. 3). Although small peaks were detectable already with 1 mg sample, only XRPD patterns from wells with ≥2 mg allowed a clear identification of CBZ crystal form I. No

differences were observed between dry and oil-wetted drug substance with respect to the intensity of XRPD signals (data not shown). Similar results were obtained for the other two model compounds, caffeine and piroxicam.

Caffeine

For the crystalline forms of caffeine (CAF) different nomenclatures have been suggested in the literature. In this work the nomenclature of Lehto and Laine (20) is employed. CAF exists as two anhydrous crystal forms (I, II) and one crystalline nonstoichiometric hydrate with 0.8 moles of water per mole of CAF (29,30). Form II of CAF, which is the stable polymorph at ambient conditions converts to form I at high temperature (20).

Initial Characterization of Caffeine Forms

Based on measured standard XRPD patterns and the patterns reported by Lehto and Laine (20), the commercial CAF was the stable form II. In DSC, CAF form II showed a shallow endothermic peak at 141.4°C (onset temperature) and a sharp endothermic peak at 235.7°C (data not shown). The first endotherm was related to the reported enantiotropic transition of CAF form II to the high-temperature form and the second endotherm to the subsequent melting of form I (20). The formation of CAF modification I after heat treatment of form II (180°C for 16 h) was confirmed by standard XRPD analysis (Fig. 4a) and by a melting point at 235.6°C in DSC. The heat-treated material showed no degradation products when analyzed by UPLC. The commercial CAF hydrate showed a weight loss step of 6.8% (w/w) in TGA analysis between 40 and 80°C upon heating, indicating a 4/5 hydrate (data not shown). The IR spectrum and the XRPD pattern of CAF hydrate (Fig. 4a) also corresponded to literature data (31).

Caffeine Solubility in Different Vehicles and Analysis of Residual Solid

The solubility of CAF forms I and II and of CAF hydrate was determined in 17 different pharmaceutical vehicles (Table I). After equilibration for 24 h at room temperature, the metastable form I of CAF was converted to the stable form II or to a mixture of form II and the hydrate in all vehicles tested. In contrast, CAF form II persisted in non-aqueous vehicles or converted to the hydrate in vehicles containing water. The kinetics of hydrate formation of CAF forms I and II differed and more CAF hydrate was found in the plate initially containing CAF form II. CAF form II in SGF, pH 2 showed substantial differences in solubility, the solubility correlating to the crystal form of the residual solids (Fig. 5). Pure CAF form II had a higher solubility in SGF, pH 2 (39.03 mg/ml) than the formed hydrate (21.59 mg/ml), the solubility of the latter being close to the one of pure CAF hydrate in SGF, pH 2 (20.89 mg/ml, mean value). The presence of small amounts of hydrate slightly reduced the solubility of CAF form II in SGF, pH 2 (37.96 mg/ml). In

Table I. Solubility of Caffeine (CAF) Polymorphs in Different Vehicles and Crystal Form of Residual Solids as Determined by HT XRPD

Crystal Form used	CAF Form I (metastable)		CAF Form II (stable)		CAF Hydrate H	
Method	SORESOS		SORESOS		SORESOS	
Vehicle	Solubility (mg/ml)[a]	Residual Solids	Solubility (mg/ml)[a]	Residual Solids	Solubility (mg/ml)[a]	Residual Solids
Untreated compound	n.a.	I	n.a.	II	n.a.	H
Buffer pH 6.5	36.10 (0.56)	II	21.45 (0.36)	H+II	20.02 (0.89)	H
SGF, pH 2	32.66 (5.36)	II+H	39.03	II	20.89 (1.72)	H
			37.96	II+H		
			21.59	H		
FaSSIF, pH 6.5	30.25 (4.45)	II+H	20.71 (0.56)	H	20.78 (1.49)	H
FeSSIF, pH 5	35.03 (1.58)	II+H	18.45 (3.93)	H	18.52 (0.36)	H
Ethanol	5.66 (0.26)	II	5.57 (0.06)	II	7.32 (0.22)	II
20% Ethanol in water (v/v)	55.16 (1.02)	II+H	52.73	II	33.14 (0.47)	H
			35.11	H+II		
			34.94	H+II		
PEG 400	12.98 (0.25)	II	12.76 (0.08)	II	12.85 (1.42)	II
20% PEG 400 in water (v/v)	29.97 (0.39)	II	18.83 (0.51)	H	17.45 (1.67)	H+II
10% HP-β-Cyclodextrine in water (w/v)	45.70 (0.53)	II+H	24.48 (1.12)	H	23.68 (0.29)	H
Mixed micelles (200 mM G/L)	29.57 (0.97)	II+H	18.16 (0.31)	H	18.06 (0.68)	H
Polysorbate 80	9.79 (0.15)	II	8.94 (0.53)	II	13.64 (0.58)	H+II
10% Polysorbate 80 in water (w/v)	35.01 (5.32)	II	21.97 (0.38)	H	20.90 (1.08)	H
Labrafil M 1944 CS	2.77 (0.51)	II	3.17 (0.05)	II	3.49 (0.20)	H+II
Labrasol	10.71 (1.79)	II	12.20 (0.18)	II	13.90 (0.47)	II
Medium chain triglycerides	1.62 (0.26)	II	1.88 (0.02)	II	2.19 (0.12)	H+II
Olive oil	0.87 (0.13)	II	0.96 (0.02)	II	1.10 (0.02)	H
Capmul MCM	11.93 (0.26)	II	11.70 (0.17)	II	13.77 (0.98)	II

[a] All measurements were performed at 25±3°C; results expressed as mean (standard error); n=3

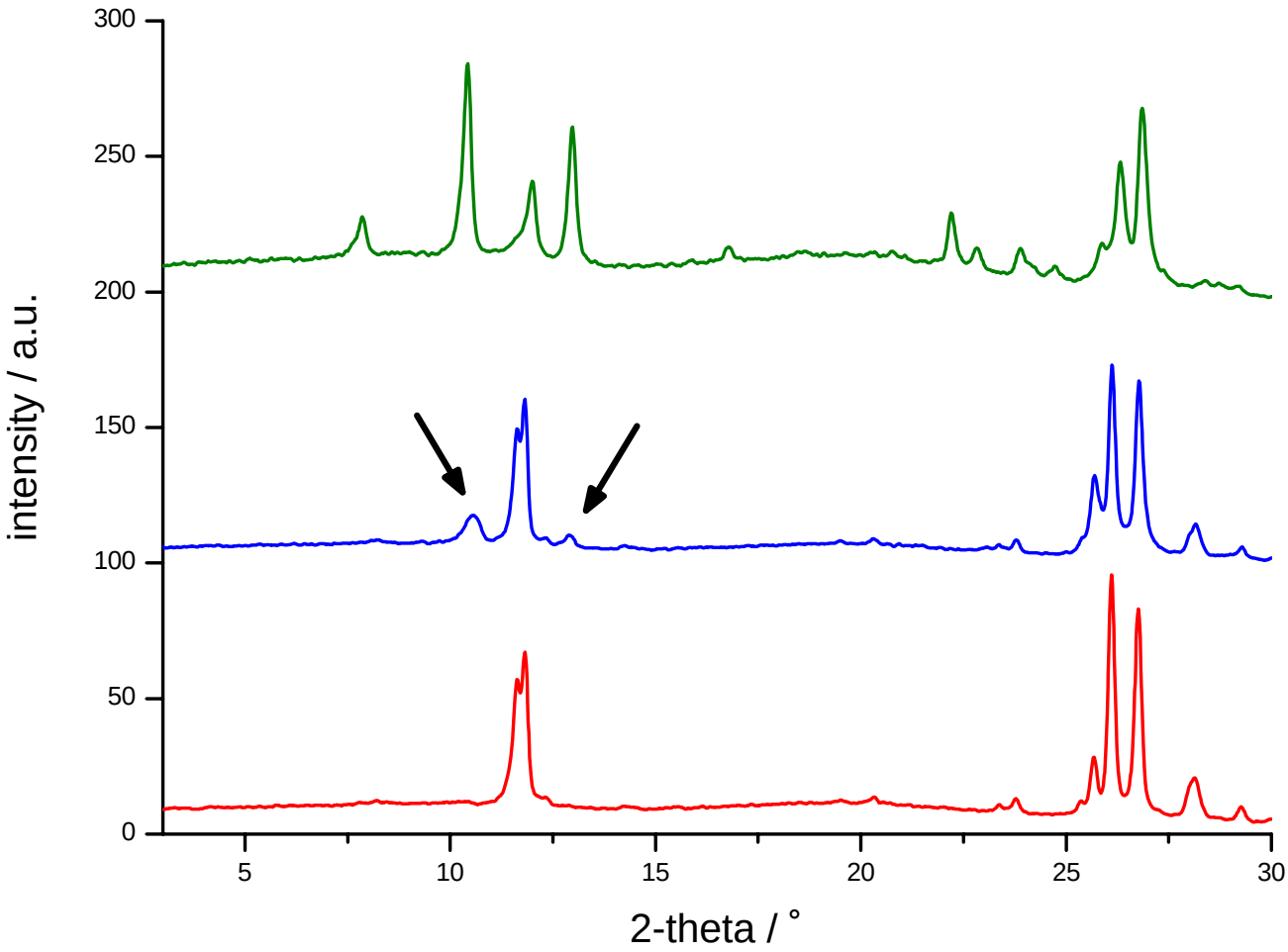

Fig. 5. Overlay of the HT XRPD patterns of residual solids of CAF form II solubility measurements in SGF, pH 2. Individual wells contained different crystal forms: form II (*bottom*), a mixture of form II and small amounts of hydrate (*middle*), or pure hydrate (*top*). Peaks that allow specific identification of the hydrate are indicated by arrows.

aqueous vehicles the solubility of anhydrous CAF (form II) was generally higher than the solubility of the hydrate. In non-aqueous vehicles such as Polysorbate 80, Labrafil M 1944 CS, medium chain triglycerides or olive oil, an inverse correlation was observed and CAF hydrate showed higher solubility. In addition, in some vehicles (e.g., ethanol, PEG 400, Labrasol, Capmul MCM) CAF hydrate was completely dehydrated to anhydrous CAF form II.

Carbamazepine

Carbamazepine (CBZ) has been analyzed in depth, however, the nomenclature of CBZ crystal forms is confusing (15,22,32). In this paper, we use the nomenclature proposed by Grzesiak *et al.* (32). Four anhydrous polymorphs, one dihydrate and several solvates of CBZ have been reported (15,21,32,33). According to Grzesiak *et al.* (32), CBZ form III is the thermodynamically most stable form at ambient temperature.

Initial Characterization of Carbamazepine Forms

Based on XRPD, IR and DSC results, the purchased CBZ was form III (32,34). The DSC thermogram exhibited a first endothermic peak at 174.1°C onset temperature, followed by an exothermic peak and a second endothermic peak at 190.0°C (data not shown). This is in good agreement with previous results, showing a transition of form III to form I at around 170°C and subsequent melting of form I at 190°C (32). CBZ form I used in this study was prepared by heating CBZ form III to 170°C for 2h and formation of form I was confirmed by XRPD, IR and DSC analysis (Fig. 4b). UPLC analysis of the heat-treated material showed no degradation products.

Carbamazepine Solubility in Different Vehicles and Analysis of Residual Solid

CBZ solubility in different vehicles is shown in Table II. The stable CBZ form III remained unchanged in non-aqueous vehicles and formed hydrates in aqueous vehicles, except for 20% PEG 400 and 10% Polysorbate 80. The metastable CBZ form I behaved almost identical but formed hydrates in all aqueous vehicles. The solubility of the hydrates was similar and independent from the starting polymorph. In 20% PEG 400 and 10% Polysorbate 80, CBZ form I converted to a mixture of the hydrate and of a new form not corresponding to form I, II, III or form IV

Table II. Solubility of Carbamazepine (CBZ) Polymorphs in Different Vehicles and Crystal Form of Residual Solids as Determined by HT XRPD (SORESOS) and Standard XRPD (large-volume solubility experiments)

Crystal Form used	CBZ Form I (metastable)		CBZ Form III (stable)		CBZ Form III (stable)	
Method	SORESOS		SORESOS		large-volume solubility experiments	
Vehicle	Solubility (mg/ml)[a]	Residual Solids	Solubility (mg/ml)[a]	Residual Solids	Solubility (mg/ml)[a,b]	Residual Solids
Untreated compound	n.a.	I	n.a.	III	n.a.	III
Buffer pH 6.5	0.10 (0.02)	H	0.13 (0.01)	H	0.10 (0.001)	H
SGF, pH 2	0.14 (0.004)	H	0.11 (0.03)	H	0.12 (0.001)	H
FaSSIF, pH 6.5	0.08 (0.003)	H	0.12 (0.02)	H	0.11 (<0.001)	H
FeSSIF, pH 5	0.14 (0.01)	H	0.20 (0.001)	H	0.17 (0.001)	H
Ethanol	23.50 (1.15)	α	27.04 (0.44)	III	23.83 (0.31)	III
20% Ethanol in water (v/v)	0.48 (0.01)	H	0.36 (0.08)	H	0.48 (0.006)	H
PEG 400	≥64.94	n.d.[c]	≥62.78	n.d.[c]	82.56 (0.69)	III
20% PEG 400 in water (v/v)	1.09 (0.04)	α+H	0.92 (0.20)	III	0.99 (0.002)	III
10% HP-β-Cyclodextrine in water (w/v)	6.48 (0.24)	H	6.18 (0.48)	H	6.30 (0.04)	H
Mixed micelles (200 mM G/L)	2.00 (0.40)	H	2.08 (0.40)	H	2.43 (0.05)	H+III
Polysorbate 80	48.03 (1.72)	I	39.93 (0.64)	III	40.94 (1.58)	III
10% Polysorbate 80 in water (w/v)	1.61 (0.38)	α+H	1.57 (0.36)	III	1.71 (0.01)	III
Labrafil M 1944 CS	8.56 (2.08)	α	7.86 (2.03)	III	10.64 (0.29)	III
Labrasol	51.26 (4.25)	α	53.15 (0.42)	III	53.36 (0.35)	III
Medium chain triglycerides	1.89 (0.06)	I	1.51 (0.07)	III	1.89 (<0.001)	III
Olive oil	1.29 (0.02)	I	1.36 (0.69)	III	1.40 (0.03)	III
Capmul MCM	53.72 (4.55)	I	48.01 (0.02)	III	50.01 (0.71)	III

[a] All measurements were performed at 25±3°C; results expressed as mean (standard error); n=3
[b] Equilibrium values after 24 h incubation
[c] Not detectable by XRPD and no residual solid observed by visual control

described by Grzesiak *et al.* (32). This was confirmed in scale-up experiments by standard XRPD measurements and comparison to the ICDD Powder Diffraction File database revealed that the new CBZ form was identical to alpha-carbamazepine (α-CBZ) originally described by Lowes *et al.* (35), ICDD-No.: 43-1998 (Fig. 6). A conversion of CBZ form I to α-CBZ was also observed in ethanol, Labrafil M 1944 CS, and Labrasol but not in Polysorbate 80, Medium chain triglycerides, olive oil, and Capmul MCM. The XRPD pattern of the CBZ hydrate formed in most aqueous vehicles was identical to the CBZ dihydrate pattern reported in the literature and to the pattern obtained in scale-up experiments (Fig. 4b) (21,36,37).

Solubility of CBZ form III determined by SORESOS was in good agreement to equilibrium solubility determined in a standard large-volume solubility experiment (Table II). In the large-volume experiments equilibrium solubility was reached after 24 h for all vehicles tested.

Piroxicam

Piroxicam (PXM) exists in at least three polymorphic forms (I, II, III) and forms a monohydrate in water (23,38). The number and nomenclature of the PXM polymorphs is not consistent and in the present study we employ the nomenclature of Sheth *et al.* (24).

Initial Characterization of Piroxicam

According to the IR and XRPD results, the purchased PXM was the form I described by Vrecer *et al.* and by Sheth *et al.* (Fig. 4c) (24,39). In DSC, PXM showed the typical endothermic peak of modification I at an onset temperature of 200.3°C (data not shown).

Piroxicam Solubility in Different Vehicles and Analysis of Residual Solid

The solubility of PXM form I in solvents is shown in Table III. In some wells, the visual change in color from white (form I) to yellow (monohydrate) already indicated the formation of a new polymorph. This was confirmed by XRPD analysis, showing that monohydrate formation occurred in almost all aqueous vehicles. Exceptions were mixed micelles (200 mM G/L) and 10% Polysorbate 80 in water that contained only PXM form I after the 24 h equilibration period. In case of buffer pH 6.5, the kinetics of hydrate formation under equal conditions differed in the triplicates. Two samples contained exclusively PXM monohydrate and one a mixture of form I and the monohydrate. The latter showed higher PXM solubility compared to the samples containing pure monohydrate. Hydrate formation was further confirmed in up-scaling experiments (Fig. 4c). The XRPD pattern corresponded to published data (39) and in TGA a weight loss of approximately 5% (w/w) was observed between 80 and 100°C upon heating (data not shown).

DISCUSSION

A number of miniaturized methods have been developed in the past to determine drug solubility in aqueous and non-aqueous vehicles. Compared to these screening assays, our combined approach allows the parallel measurement of

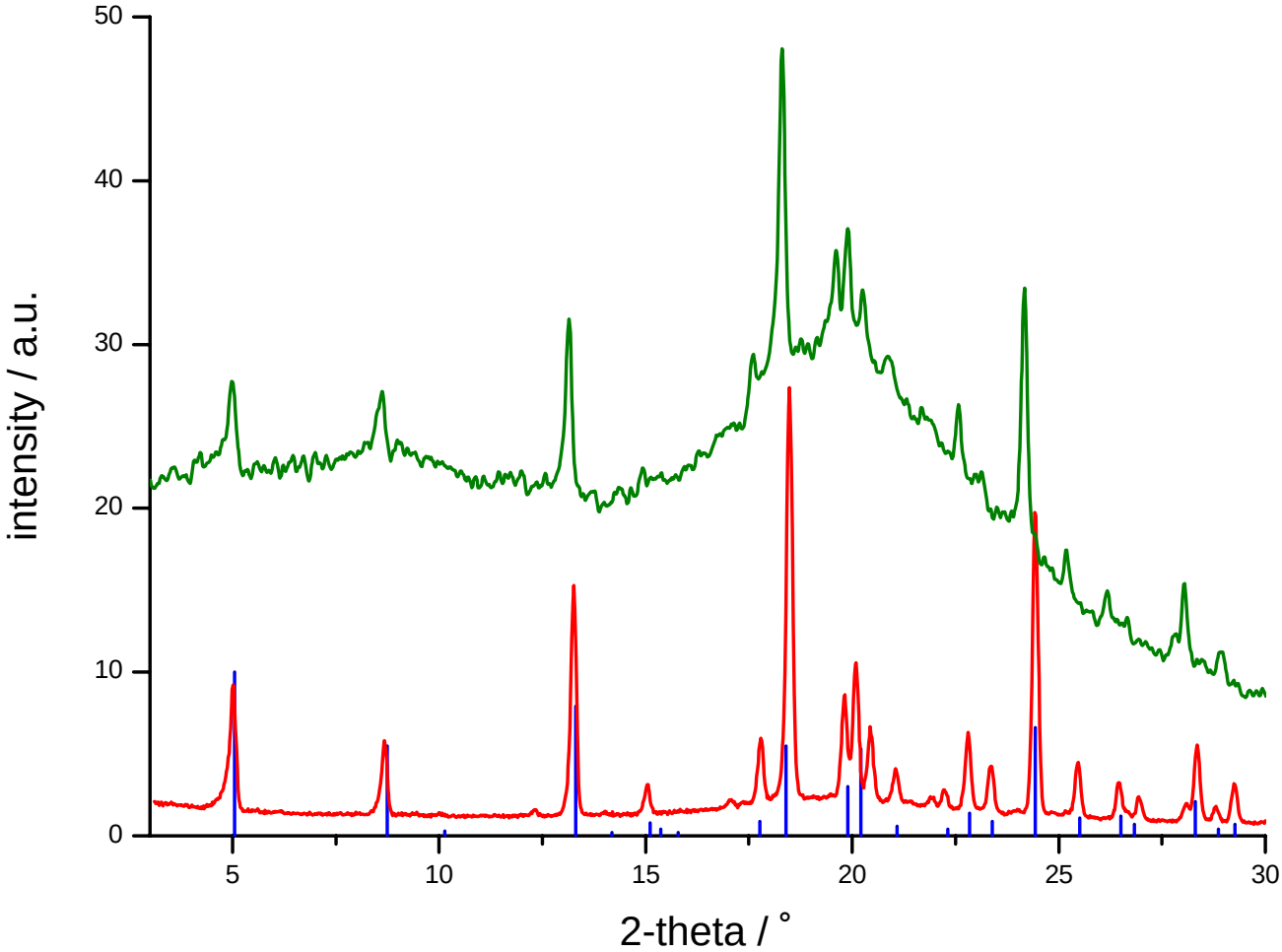

Fig. 6. XRPD patterns of **α**-CBZ: ICDD reference (*bottom*), scale-up reference (*middle*), and HT XRPD pattern (*top*).

solubility and solid form modifications during solubility studies in a single assay. The assay is a 96-well solubility assay that has a medium throughput, is easy to perform, uses only minimum amounts of drug substance, and allows the determination of polymorph specific solubility in pharmaceutical vehicles.

The importance of a simultaneous characterization of residual solid to obtain high quality solubility data has been shown using CAF, CBZ and PXM as model compounds. Depending on the crystal form of the starting material and on the vehicle used, solid form conversions have been detected in our solubility studies. The detection of these conversions explained the solubility differences seen in some replicates and allowed to attribute drug solubility values to a specific polymorph (Tables I and III). Interestingly, CAF hydrate showed higher solubility in non-aqueous vehicles (e.g., Polysorbate 80 or Labrasol) compared to the anhydrous forms (Table I). This observation could be explained by partial (Polysorbate 80, Labrafil M 1944 CS, medium chain triglycerides) or complete dehydration (Labrasol, Capmul MCM, ethanol) of the hydrate which increases the water content in non-aqueous solvents (15 mg of CAF hydrate can potentially release ~1 mg of water, corresponding to ~1% of water in a 100 µl sample) and may influence the solubility of the compound. The total effect will depend on the amount of solid added, on the solubility and on the degree of hydration of the compound.

HT solubility results of CBZ form III determined by SORESOS are in good agreement to equilibrium solubility determined with a standard large-volume solubility test (Table II). Overall, our solubility results are also in good agreement with published data (7,40–43) and are in line with a recent literature survey showing that the ratios of polymorph solubility are typically less than 2 (44). Compared to the PASS assay (7), the drug-vehicle mixtures in the SORESOS assay are directly equilibrated in the filter plate and hence a sample transfer to filters is not necessary prior to phase separation. For low solubility compounds, this set-up also has the advantage that the membranes are already saturated during the equilibration phase and pre-rinsing of the filters is not necessary. Preliminary results indicated that mechanical mixing of the drug-vehicle blends is essential to ensure complete mixing of the components during equilibration, particularly when viscous vehicles such as oils or pure surfactants are used. First experiments revealed that magnetic stirring for 24 h caused abrasion of the filter membranes resulting in a burst of the membranes during centrifugation or by using a vacuum manifold. For that reason mixing of the samples was accomplished by addition of stirring bars to the drug-vehicle slurry and by head-over-head rotation. This technique assured a complete mixing of the samples with only minimum mechanical stress for the membranes.

Table III. Solubility of Piroxicam (PXM) in Different Vehicles and Crystal Form of Residual Solids as Determined by HT XRPD

Crystal Form used	PXM Form I (stable)	
Method	SORESOS	
Vehicle	Solubility (mg/ml)[a]	Residual Solids
Untreated compound	n.a.	I
Buffer pH 6.5	0.276	I+H
	0.072	H
	0.084	H
SGF, pH 2	0.05 (0.003)	I+H
FaSSIF, pH 6.5	0.36 (0.03)	I+H
FeSSIF, pH 5	0.12 (0.02)	I+H
Ethanol	1.35 (0.01)	I+H
20% Ethanol in water (v/v)	0.02 (0.001)	H
PEG 400	20.07 (0.19)	I+H
20% PEG 400 in water (v/v)	0.07 (0.03)	H
10% HP-β-Cyclodextrine in water (w/v)	0.32 (0.02)	I+H
Mixed micelles (200 mM G/L)	0.64 (0.02)	I
Polysorbate 80	14.96 (0.23)	I
10% Polysorbate 80 in water (w/v)	0.44 (0.004)	I
Labrafil M 1944 CS	2.34 (0.12)	I+H
Labrasol	13.60 (0.77)	I
Medium chain triglycerides	1.88 (0.14)	I
Olive oil	0.73 (0.01)	I
Capmul MCM	6.04 (0.36)	I

[a] All measurements were performed at 25±3°C; results expressed as mean (standard error); n=3

In the new assay, residual solid analysis is performed by HT XRPD measurement. XRPD is generally regarded as "gold standard" for solid form analysis (17). However, preliminary experiments demonstrated that Raman microscopy might also be an option, especially at very low amounts of sample. In our experiments, HT XRPD analysis was not affected by liquid excipients remaining on the surface of solid particles after filtration. Therefore, no additional preparation step was needed after filtration and the plates could directly be transferred to HT XRPD analysis. To detect distinct XRPD signals, approximately 2–5 mg of residual solid per well is required. The adhesive acetate foil used to seal the plate after filtration ensured that the solid residues were kept wet during solid state analysis to avoid drying related recrystallization. In early development, reference XRPD patterns of well characterized crystal forms of a drug are often not available. In these cases, HT XRPD results can still be used to track changes in the solid form during solubility experiments and help to relate solubility data to crystal forms and thus explain deviations in, for example, replicates (Tables I and III). Of course, a single characterization method is scarcely sufficient in solid state analysis and multiple analytical techniques should be employed after scale-up of respective samples to fully characterize new crystal forms.

The quality of the HT XRPD data is less compared to patterns obtained from a standard transmission XRPD method where every sample is prepared individually and a single analysis takes approximately 60 min. The observed broadening of peaks results from the lower angular resolution of the imaging plate detector and the "non-ideal" preparation for HT XRPD analytics. The polycarbonate membrane of the filtration plate gives rise to an amorphous halo resulting in poorer signal to noise ratio compared to the standard transmission XRPD method. Whereas for in depth analysis of an XRPD pattern (e.g., indexing of peaks, determination of size and strain) excellent angular resolution is required the quality requirements are less for high-throughput qualitative phase analysis (45). The HT transmission XRPD method described in this paper enables reliable qualitative analysis of the residual solid and gives a good picture of its crystallinity and the solid form changes occurring during solubility studies.

The parallel measurement of solubility and of crystal form opens new perspectives to the formulator for the selection of vehicles for preclinical studies. The conversion of a compound into a less soluble hydrate for example can be easily identified and certain vehicles or excipients inhibiting this process might also be identified early on. This could facilitate the selection of excipients that stabilize the physical form of drugs in formulations and hence ensure adequate oral bioavailability of poorly soluble compounds. An example reported in the literature is the inhibition of the phase transition of the anhydrous form of metronidazole benzoate to the monohydrate in aqueous suspensions in the presence of β-cyclodextrin (46). Finally, in early drug development where often amorphous material or metastable crystalline solid is used, the assay allows the easy identification of recrystallization processes during solubility studies and gives first hints on potential polymorphism issues of the tested drug.

CONCLUSION

A new miniaturized, combined method for the measurement of drug solubility and for the screening of residual solid in 96-well filter plates is presented. The assay works in aqueous and non-aqueous pharmaceutical vehicles at a 100 µl scale, consumes only minimal amounts of drug substance, and is well suited for high-throughput experimentation and automation. The method is intended for pharmaceutical profiling of new drug compounds in the late lead optimization and clinical candidate selection phase. It will speed-up the identification of promising formulation approaches for non-clinical *in vivo* studies, facilitate the estimation of the formulation potential of a drug candidate for clinical development, and help to detect potential polymorphism of a compound early on.

ACKNOWLEDGMENTS

The authors wish to thank Annunziato Raso for UPLC measurements, Dorothea Held and Sabine Schwarz for standard XRPD analyses, and André Bubendorf for IR spectroscopy studies.

REFERENCES

1. S. Venkatesh and R. A. Lipper. Role of the development scientist in compound lead selection and optimization. *J. Pharm. Sci.* **89**:145–154 (2000).

2. G. W. Caldwell, D. M. Ritchie, J. A. Masucci, W. Hageman, and Z. Yan. The new pre-clinical paradigm: compound optimization in early and late phase drug discovery. *Curr. Topics Med. Chem.* **1**:353–366 (2001).
3. E. H. Kerns. High throughput physicochemical profiling for drug discovery. *J. Pharm. Sci.* **90**:1838–1858 (2001).
4. S. Balbach and C. Korn. Pharmaceutical evaluation of early development candidates "the 100 mg-approach". *Int. J. Pharm.* **275**:1–12 (2004).
5. H. Chen, Z. Zhang, C. McNulty, C. Olbert, H. J. Yoon, J. W. Lee, S. C. Kim, M. H. Seo, H. S. Oh, A. V. Lemmo, S. J. Ellis, and K. Heimlich. A high-throughput combinatorial approach for the discovery of a cremophor EL-free paclitaxel formulation. *Pharm. Res.* **20**:1302–1308 (2003).
6. X.-Q. Chen and S. Venkatesh. Miniature device for aqueous and non-aqueous solubility measurements during drug discovery. *Pharm. Res.* **21**:1758–1761 (2004).
7. J. Alsenz, E. Meister, and E. Haenel. Development of a partially automated solubility screening (PASS) assay for early drug development. *J. Pharm. Sci.* **96**:1–15 (2007).
8. M. E. Swartz. UPLC™: An introduction and review. *J. Liquid Chromatogr. Relat. Technol.* **28**:1253–1263 (2005).
9. L. Nováková, L. Matysová, and P. Solich. Advantages of application of UPLC in pharmaceutical analysis. *Talanta* **68**:908–918 (2006).
10. A. Bauer-Brandl. Polymorphic transitions of cimetidine during manufacture of solid dosage forms. *Int. J. Pharm.* **140**:195–206 (1996).
11. G. W. Lu, M. Hawley, M. Smith, B. M. Geiger, and W. Pfund. Characterization of a novel polymorphic form of Celecoxib. *J. Pharm. Sci.* **95**:305–317 (2006).
12. S. R. Vippagunta, H. G. Brittain, and D. J. W. Grant. Crystalline solids. *Adv. Drug. Del. Rev.* **48**:3–26 (2001).
13. C. R. Gardner, C. T. Walsh, and Ö. Almarsson. Drugs as materials: valuing physical form in drug discovery. *Nature Reviews. Drug Discovery* **3**:926–934 (2004).
14. M. L. Peterson, S. L. Morissette, C. McNulty, A. Goldsweig, P. Shaw, M. LeQuesne, J. Monagle, N. Encina, J. Marchionna, A. Johnson, J. Gonzalez-Zugasti, A. V. Lemmo, S. J. Ellis, M. J. Cima, and Ö. Almarsson. Iterative high-throughput polymorphism studies on acetaminophen and an experimentally derived structure for form III. *J. Am. Chem. Soc.* **124**:10958–10959 (2002).
15. R. Hilfiker, J. Berghausen, F. Blatter, A. Burkhard, S. M. PaulDe, B. Freiermuth, A. Geoffroy, U. Hofmeier, C. Marcolli, B. Siebenhaar, M. Szelagiewicz, A. Vit, and M. Raumervon. Polymorphism—integrated approach from high-throughput screening to crystallization optimization. *J. Therm. Anal. Cal.* **73**:429–440 (2003).
16. P. J. Desrosiers. The potential of preform. *Mod. Drug Discov.* **7**:40–43 (2004).
17. R. Storey, R. Docherty, P. Higginson, C. Dallman, C. Gilmore, G. Barr, and W. Dong. Automation of solid form screening procedures in the pharmaceutical industry—how to avoid the bottlenecks. *Cryst. Rev.* **10**:45–56 (2004).
18. S. E. Rasmussen. Relative merits of reflection and transmission techniques in laboratory powder diffraction. *Powder Diffr.* **18**:281–284 (2003).
19. A. J. Florence, B. Baumgartner, C. Weston, N. Shankland, A. R. Kennedy, K. Shankland, and W. I. F. David. Indexing powder patterns in physical form screening: instrumentation and data quality. *J. Pharm. Sci.* **92**:1930–1938 (2003).
20. V.-P. Lehto and E. Laine. A kinetic study of polymorphic transition of anhydrous caffeine with microcalorimeter. *Thermochim. Acta* **317**:47–58 (1998).
21. F. U. Krahn and J. B. Mielck. Relations between several polymorphic forms and the dihydrate of carbamazepine. *Pharm. Acta Helv.* **62**:247–254 (1987).
22. R. J. Behme and D. Brooke. Heat of fusion measurement of a low melting polymorph of carbamazepine that undergoes multiple-phase changes during differential scanning calorimetry analysis. *J. Pharm. Sci.* **80**:986–990 (1991).
23. F. Vrecer, S. Srcic, and J. Smid-Korbar. Investigation of piroxicam polymorphism. *Int. J. Pharm.* **68**:35–41 (1991).
24. A. R. Sheth, S. Bates, F. X. Muller, and D. J. W. Grant. Polymorphism in Piroxicam. *Cryst. Growth Des.* **4**:1091–1098 (2004).
25. E. Galia, J. Horton, and J. B. Dressman. Albendazole Generics—a comparative *in vitro* study. *Pharm. Res.* **16**:1871–1875 (1999).
26. E. Galia, E. Nicolaides, C. Reppas, and J. B. Dressman. New media discriminate dissolution of poorly soluble drugs. *Pharm. Res.* **13**:S-262, 1996 (1996).
27. K. Teelmann, B. Schläppi, M. Schüpbach, and A. Kistler. Preclinical safety evaluation of intravenously administered mixed micelles. *Arzneim.-Forsch./Drug Res.* **34**:1517–1523 (1984).
28. C. Lefebvre, A. M. Guyot-Hermann, M. Draguet-Brughmans, R. Bouché, and J. C. Guyot. Polymorphic transitions of carbamazepine during grinding and compression. *Drug Dev. Ind. Pharm.* **12**:1913–1927 (1986).
29. H. Bothe and H. K. Cammenga. Composition, properties, stability and thermal dehydration of crystalline caffeine hydrate. *Thermochim. Acta* **40**:29–39 (1980).
30. U. J. Griesser and A. Burger. The effect of water vapor pressure on desolvation kinetics of caffeine 4/5 hydrate. *Int. J. Pharm.* **120**:83–93 (1995).
31. A. Jorgensen, J. Rantanen, M. Karjalainen, L. Khriachtchev, E. Räsänen, and J. Yliruusi. Hydrate formation during wet granulation studied by spectroscopic methods and multivariante analysis. *Pharm. Res.* **19**:1285–1291 (2002).
32. A. L. Grzesiak, M. Lang, K. Kim, and A. J. Matzger. Comparison of the four anhydrous polymorphs of carbamazepine and the crystal structure of form I. *J. Pharm Sci.* **92**:2260–2271 (2003).
33. M. Lang, J. W. Kampf, and A. J. Matzger. Form IV of carbamazepine. *J. Pharm. Sci.* **91**:1186–1190 (2002).
34. V. L. Himes, A. D. Mighell, and W. H. CampDe. Structure of Carbamazepine: 5H-Dibenz[b,f]azepine-5-carboxamide. *Acta Cryst.* **B37**:2242–2245 (1981).
35. M. M. J. Lowes, M. R. Caira, A. P. Lötter, and J. G. WattVan Der. Physicochemical properties and X-ray structural studies of the trigonal polymorph of carbamazepine. *J. Pharm. Sci.* **76**:744–752 (1987).
36. L. E. McMahon, P. Timmins, A. C. Williams, and P. York. Characterization of dihydrates prepared from carbamazepine polymorphs. *J. Pharm. Sci.* **85**:1064–1069 (1996).
37. G. Reck and G. Dietz. The order-disorder structure of carbamazepine dihydrate: 5H-dibenz[b,f]azepine-5-carboxamide dihydrate, C15H12N2O.2 H2O. *Cryst. Res. Technol.* **21**:1463–1468 (1986).
38. F. Kozjek and L. Golic. Physico-chemical properties and bioavailability of two crystal forms of piroxicam. *Acta Pharm. Jugosl.* **35**:275–281 (1985).
39. F. Vrecer, M. Vrbinc, and A. Meden. Characterization of piroxicam crystal modifications. *Int. J. Pharm.* **256**:3–15 (2003).
40. D. Roy, F. Ducher, A. Laumain, and J. Y. Legendre. Determination of the aqueous solubility of drugs using a convenient 96-well plate-based assay. *Drug Dev. Ind. Pharm.* **27**:107–109 (2001).
41. M. Yazdanian, K. Briggs, C. Jankovsky, and A. Hawi. The "High Solubility" definition of the current FDA guidance on biopharmaceutical classification system may be too strict for acidic drugs. *Pharm. Res.* **21**:293–299 (2004).
42. K. Obata, K. Sugano, M. Machida, and Y. Aso. Biopharmaceutics classification by high throughput solubility assay and PAMPA. *Drug Dev. Ind. Pharm.* **30**:181–185 (2004).
43. R.-K. Chang and A. H. Shojaei. Effect of hydroxypropyl β-cyclodextrin on drug solubility in water-propylene glycol mixtures. *Drug Dev. Ind. Pharm.* **30**:297–302 (2004).
44. M. Pudipeddi and A. T. M. Serajuddin. Trends in solubility of polymorphs. *J. Pharm. Sci.* **94**:929–939 (2005).
45. J. I. Langford. Line profile analysis: a historical overview. *Springer Ser. Mat. Sci.* **68**:3–13 (2004).
46. F. M. Andersen and H. Bundgaard. Inclusion complexation of metronidazole benzoate with β-cyclodextrin and its depression of anhydrate-hydrate transition in aqueous suspension. *Int. J. Pharm.* **19**:189–197 (1984).